

Gain Scheduling Based PID Control Approaches for Path Tracking and Fault Tolerant Control of a Quad-rotor UAV

Jing Qiao, Zhixiang Liu, and Youmin Zhang¹

Concordia University, Montreal, H3G 1M8, Quebec, Canada

Email: josephchiao@163.com*, lzhx180@gmail.com, ymzhang@encs.concordia.ca

Abstract—Quad-rotor UAVs have generated considerable interest in the control community because of their wide applications due to their advantages over regular air vehicles. In this paper Gain-Scheduling PID (GS-PID) control approaches were designed for a quad-rotor UAV with the feature of being a multivariable nonlinear system. The control target, a Quanser Qball-X4 quad-rotor UAV, was introduced in this paper. The proposed design procedure of control approaches is based on the parameter dependent quadratic stability approach. The mission processes includes a programmed path tracking of the quad-rotor, and a fault-tolerant process of the quad-rotor during hovering. Simulation results carried out are shown, wherein the performance achieved with these control strategies are shown as well. The simulation results show that control algorithms implemented for the quad-rotor UAV in this paper could increases the performance of the quad-rotor UAV in tracking the desired trajectory and increases reliability of the UAV.

Index Terms—Quad-rotor, UAV, PID controller, gain scheduling, trajectory tracking, fault tolerant

I. INTRODUCTION

Unmanned Aerial Vehicle (UAV) is a special kind of aircraft, which can fly independently or controlled via remote signals. In recently years, due to the increasing military and civilian requirements, the rotor craft UAV has become most popular. Especially, with the continuous development of microelectronics technology in recent years, quad-rotor UAV achieved rapid development, and it has been widely applied in aerial photography, remote sensing, environmental monitoring, disaster relief, public security, fire alarming, anti-terrorism, cinematography, express delivery and other related areas due to its advantages including flexible control, low cost, etc. [1, 2, 3].

However, the flight control of rotor craft UAV has brought challenges to researchers. Since the quad-rotor UAV is a typical non-linear, strong coupling, under-actuated and multi-input and multi-output complex system, and all these make its control design complicated. This has motivated the research and development of new control systems for the applications of UAV. A lot of researches have been carried out in a wide range of fields

in control, such as computer vision feedback, fusion sensor, and linear and nonlinear control methodologies to improve performance of this kind of system. Equations of motions for quad-rotor UAV can be found in [4], [5]. These equations can be used for the control of the quad-rotor UAV by means of many control strategies, such as MPC, H1, and PID [6],[7],[8]. Feedback information can be provided by inertial measurement units, GPS, or even computer vision systems [9].

Proportional-Integral-Derivative (PID) controllers are the most widely used controllers in various industries. PID controllers are also reliable and easy to use for most industrial applications [10]. However, classical PID control sometimes can not meet the flight safety of the aircraft in special circumstances when the parameters or the state of the UAV change rapidly, such as UAV with a flight mission of payload dropping, or flying at abnormal state. In recent years, professor Zhang in Concordia University proposed to use Gain-Scheduling based PID (GS-PID) controller for fault tolerant control (FTC) and payload drop application of a quad-rotor UAV [11,12]. It is known that GS-PID is a versatile technique which can be used for situations in which the parameters or the operating conditions of the plant can change largely and rapidly [13, 14]. In aerospace applications, different portions of the flight envelope must be considered in control system design for different flight conditions. Various phases of flight need proper tuning of the controller gains under different flight conditions [15,16].

In view of popularity of GS-PID and advantages of such simple and model-free control design strategy, a GS-PID controller that assumes a separate set of gains for an actuator fault injected procedure is designed and implemented for the fault tolerant control of a quad-rotor UAV during its hovering in this paper. The interpolation algorithm is also used to optimize the Gain Scheduling PID tuning process, which reduces the workload of GS-PID controller tuning, as well as optimizes the fault-tolerant control performance. The proposed control law stabilize the quad-rotor UAV system and drive the system states, including three-dimensional positions and yaw angle to track the desired path, while keep the closed loop system stable.

The sections of the paper is organized as follows. Section 2 describes the model of quad-rotor used in this

Manuscript received Sept. 25, 2017; revised July 1, 2018.

study. In Section 3, the controller structure and the system parameters are explained. Simulation results are presented in Section 4, and finally conclusions and future works are drawn in Section 5.

II. SYSTEM MODELING

A. Qball-X4 Quad-rotor UAV

The quad-rotor UAV which is as the object of this study is the Qball-X4 [17] as shown in Fig. 1 which is at the Network Autonomous Vehicle (NAV) Lab in the Department of Mechanical and Industrial Engineering of Concordia University and was developed by Quanser Inc. partially under the financial support of NSERC (Natural Sciences and Engineering Research Council of Canada) in association with an NSERC Strategic Project Grant led by Concordia University since 2007. The quad-rotor UAV is enclosed within a protective carbon fiber ball-shape cage (therefore a name of Qball-X4) to ensure safe operation. It uses four 10*4.7 inch propellers and standard RC motors and speed controllers.

The motors of the Qball-X4 are out-runner brushless motors. The generated thrust T_i of the *No.i* motor is related to the Pulse Width Modulation (PWM) input u_i by a first-order linear transfer function as follows:

$$T_i = k \frac{\omega}{s + \omega} u_i \quad (1)$$

where $i = 1, 2, 3, 4$ and k is a positive gain and ω is the motor bandwidth. k and ω are theoretically the same for the four motors but this may not be the case in practice. It should be noted that $u_i=0$ corresponds to zero thrust and $u_i=0.05ms$ corresponds to the maximal thrust that can be generated by the *No.i* motor.



Figure 1. The Qball-X4 quad-rotor UAV

The block diagram of the UAV system is illustrated in Fig. 2. It is composed of three main parts. The first part represents the Electronic Speed Controllers (ESCs), the motors, and the propellers in a set of four. The input to this part is $u=[u_1, u_2, u_3, u_4]^T$ which are Pulse Width Modulation (PWM) signals. The output is the thrust vector $T=[T_1, T_2, T_3, T_4]^T$ generated by four individually-controlled motor-driven propellers. The second part is the geometry that relates the generated thrusts to the

applied lift and torques to the system. This geometry corresponds to the position and orientation of the propellers with respect to the center of mass of the Qball-X4. The third part is the dynamics that relate the applied lift and torques to the position (P), velocity (V) and acceleration (A) of the Qball-X4.

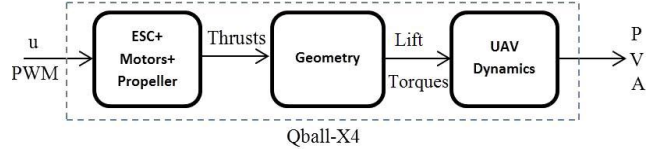


Figure 2. The UAV system block diagram

B. System Modeling

Modeling a vehicle such as a quad-rotor is not an easy task because of its complex structure. Our aim is to develop a model of the vehicle as realistically as possible. A quad-rotor is an under actuated aircraft with fixed pitch angle as shown in Fig. 3. Having Quad-Rotor with fixed angles makes quad-rotor has four input forces which are basically the thrust provided by each propellers. The motors and propellers are configured in such a way that the back and front (1 and 2) motors spin clockwise (thus inducing two counterclockwise torques on the body) and the left and right (3 and 4) spin counterclockwise (thus inducing two clockwise torques on the body). Each motor is located at a distance L from the center of mass O (0.2 m) and when spinning, a motor produces a torque τ_i which is in the opposite direction of motion of the motor as shown in Fig. 3. Forward (backward) motion is maintained by increasing (decreasing) speed of front (rear) rotor speed while decreasing (increasing) rear (front) rotor speed simultaneously which means changing the pitch angle. Left and right motion is accomplished by changing roll angle by the same way. The front and rear motors rotate counter-clockwise while other motors rotate clockwise so yaw command is derived by increasing (decreasing) counter-clockwise motors speed while decreasing (increasing) clockwise motor speeds.

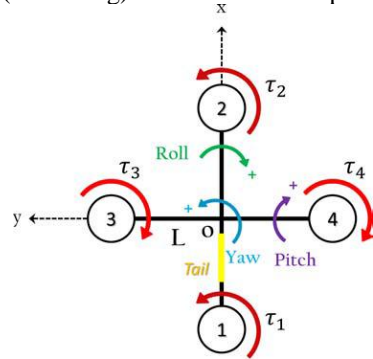


Figure 3. Schematic representation of the Qball-X4

The origin of the body-fixed frame is the system's center of mass O with the x-axis pointing from back to front and the y-axis pointing from right to left. The thrust T_i generated by the i^{th} propeller is always pointing upward in the z-direction in parallel to the motor's rotation axis. The thrusts T_i and the torques τ_i result in a lift in the z-

direction (body-fixed frame) and torques about the x-, y- and z-axis.

The relations between the lift/torques and the thrusts are

$$\begin{aligned} u_z &= T_1 + T_2 + T_3 + T_4 \\ u_\theta &= L(T_1 - T_2) \\ u_\phi &= L(T_3 - T_4) \\ u_\psi &= \tau_1 + \tau_2 - \tau_3 - \tau_4 \end{aligned} \quad (2)$$

The torque τ_i produced by the i^{th} motor is directly related to the thrust T_i via the relation of $\tau_i = K_{\psi}T_i$ with K as a constant. In addition, by setting $T_i = Ku_i$ the above relations can be written in a compact matrix form as:

$$\begin{bmatrix} u_z \\ u_\theta \\ u_\phi \\ u_\psi \end{bmatrix} = \begin{bmatrix} K & K & K & K \\ KL - KL & 0 & 0 & 0 \\ 0 & 0 & KL - KL & -KL \\ KK_\psi & KK_\psi - KK_\psi & -KK_\psi & KK_\psi \end{bmatrix} \begin{bmatrix} u_1 \\ u_2 \\ u_3 \\ u_4 \end{bmatrix} \quad (3)$$

where u_z is the total lift generated by the four propellers and applied to the quad-rotor UAV in the z-direction (body fixed frame). u_θ , u_ϕ and u_ψ are respectively the applied torques in θ , ϕ and ψ - directions (see Fig. 3). L is the distance from the center of mass to each motor.

Because many control design methods can still keep good performance with the parameter uncertainty in the model, it is acceptable with reasonable model simplification. A commonly employed quad-rotor UAV model is:

$$\begin{aligned} \ddot{x} &= u_1(\cos\phi\sin\theta\cos\psi + \sin\phi\sin\psi) - K_1\dot{x}/m \\ \ddot{y} &= u_1(\sin\psi\sin\theta\cos\phi - \cos\psi\sin\phi) - K_2\dot{y}/m \\ \ddot{z} &= u_1\cos\phi\cos\theta - g - K_3\dot{z}/m \\ \ddot{\phi} &= u_2 - lK_4\dot{\phi}/J_1 \\ \ddot{\theta} &= u_3 - lK_5\dot{\psi}/J_2 \\ \ddot{\psi} &= u_4 - lK_6\dot{\phi}/J_3 \end{aligned} \quad (4)$$

The (x, y, z) is the system position, (ϕ , θ , ψ) is respectively the rolling angle, pitch angle and yaw angle. g is the gravity acceleration, l is the distance from the center of the rotor to the rotor; the m is mass, J_i ($i=1,2,3$) represents the going inertia relative to the shaft. K_i is the constant associated with the traction coefficient. u_i is Virtual control input, the expression is respectively as,

$$\begin{aligned} u_1 &= (F_1 + F_2 + F_3 + F_4)/m \\ u_2 &= L(F_4 - F_2)/J_1 \\ u_3 &= L(F_3 - F_2)/J_2 \\ u_4 &= C(F_1 - F_2 + F_3 - F_4)/J_3 \end{aligned} \quad (5)$$

F_i ($i=1,2,3,4$) is the forces generated by Quad-Rotors, C is a coefficient.

The model used in this paper does not take into account the interference, and if the interference is taken into account, it becomes more complex and the controller design is more difficult.

III. CONTROLLER DESIGN

A. The Algorithm of the PID Controller

The key idea of PID control algorithm is to eliminate the deviation according to the deviation. The algorithm

can predict the future of the control system in the past, the present and the controlled system effectively. Control systems are usually composed of system set values, controlled objects, and PID controllers. The structure of the PID control system is shown in figure 4. According to the figure, the system consists of two parts, the forward channel and the feedback channel. The output of the controlled object $y(t)$ is used as the input of the feedback channel. The value and control system for a given value of $y_d(t)$ value of the deviation control system (error), $error(t) = y_d(t) - y(t)$, the deviation by proportional integral differential three after adding $u(t)$ as a controlled object input.

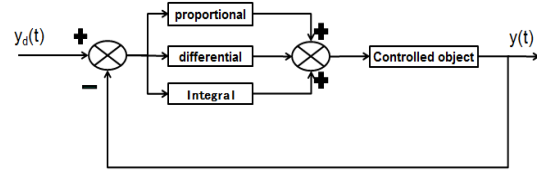


Figure 4. Structure of PID control system

The PID algorithm for $u(t)$ follows the following procedure:

$$u(t) = K_p \left[error(t) + \frac{1}{T_i} \int_0^t error(t)dt + \frac{T_d derror(t)}{dt} \right] \quad (6)$$

Transfer function is obtained after Laplace transformation of formula:

$$G(s) = \frac{u(s)}{error(s)} = K_p \left(1 + \frac{1}{T_i s} + T_d s \right) \quad (7)$$

The above two equations are the form of expression of PID control algorithm and is the most commonly used type, K_p or T_i , to gain proportional coefficient integral time constant, T_d differential time constant, PID, PI, PD can be P or PID, in all of the PID controller is an indispensable part. The three parameters of K_p , T_i and T_d in PID controller are different to the system.

Increasing the scale factor K_p can speed up the system's response speed, increase the system's control accuracy and reduce the static error of the system, but it could not completely eliminate the static error of the system. Increase the integral time constant T_i , integral effect is reduced, the control system overshoot, oscillation frequency reduction, the system more stable, but will lengthen the system to eliminate static error, reduce the integral time constant has the opposite effect. When the differential time constant T_d is increased, the response speed of the system increases, the overshoot decreases, and the stability increases, but too much will cause the system to suppress the disturbance. In the actual control system, according to the specific requirements of the control system, the three parameters are dynamically adjusted until the performance requirements of the control system are met.

The algorithm of the PID controller for discrete version is shown as following:

$$u(t_k) = u(t_{k-1}) + \Delta u(t_k) \quad (8)$$

where

$$\Delta u(t_k) = K_p [e(t_k) - e(t_{k-1})] + \frac{K_p h}{T_i} e(t_k) + \frac{K_p T_d}{h} [e_f(t_k) - 2e_f(t_{k-1}) + e_f(t_{k-2})] \quad (9)$$

where u is the control variable, h is discretization rate, e is the tracking error defined as $e = y_d - y$ where y_d is the desired output and y is the real output of the system. K_p , $K_i = K_p/T_i$, and $K_d = K_p * T_d$ are controller gains associated with proportional (P), integral (I), and derivative (D) action, respectively.

B. Gain Scheduling Control Approach

Generally, if the change of dynamics in a system/process with the operating condition is known, it is possible to change the parameters of the controller by monitoring the operating conditions of the process. This approach is gain scheduling, because the scheme was originally used to accommodate changes in process gain only. A block figure of a control system with gain scheduling mechanism is shown in Fig. 5.

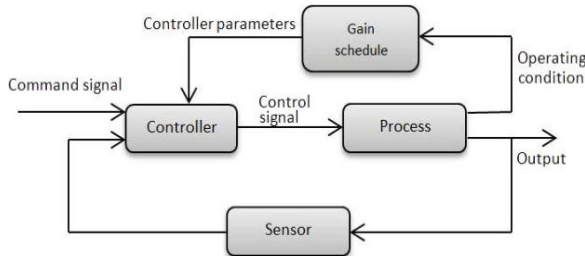


Figure 5. Gain scheduling control structure

The idea of relating the controller parameters to auxiliary variables is not new, but the implementation of gain scheduling is still challenging in practice. In this paper, with the aim of fault-tolerant control of the Quadrotor UAV while an actuator fault is injected during hovering period, the interpolation algorithm is used to optimize the Gain Scheduling PID tuning process. A set of pre-tuned PID controller gains are applied to the controllers for expected fault occurrences or for situations in which the parameters or the operating conditions of the UAV can change largely and rapidly. Under the assumption that a fault detection and diagnosis module can detect and identify the fault quick and correctly, this control scheme can be used for switching pre-tuned PID controllers for obtaining best performance for each considered fault case. Based on these considerations, the Gain Scheduling based PID control approach was used in this paper by exploiting the advantages for PID controllers and gain scheduling control strategy[11].

But a general rate of control with gain scheduling algorithm has yet to be realized. Each fault case or parameter change must be handled separately. In order to overcome this limitation, the interpolation algorithm is used to optimize the gain scheduling control in this study. Assume that proper controller gains of the PID controllers have been found for different situations, these

values can be stored in a parameter table which will be picked based on a gain scheduling variable based on the different fault types and magnitudes. In the actual operation of the system, the region of the compensator is determined according to the situation. When different faults occur, the PID controllers will be switched to the corresponding fault case, and the parameters of the compensator are determined by interpolation between the operation points. With the gain scheduling table, the PID parameter can be reset by interpolation method according to different fault.

To acquire different gains, La Grange formula can be used for the interpolation algorithm.

$$K = \sum_{i=1}^N \left[K \prod_{j=1, j \neq i}^N \frac{f - f_j}{f_i - f_j} \right] \quad (10)$$

where K is controller gains associated with proportional (P), integral (I), and derivative (D) actions respectively. f is the failure rate parameter for specified fault types. The subscript i and j are the specified failure rate in the parameter table.

C. System Parameters

In this paper, a simulation module of Quad-rotor UAV is built by Matlab/Simulink, and system simulation is carried out to verify the expected result of GS-PID controller. The sketch map of the simulation system designed is as follows.

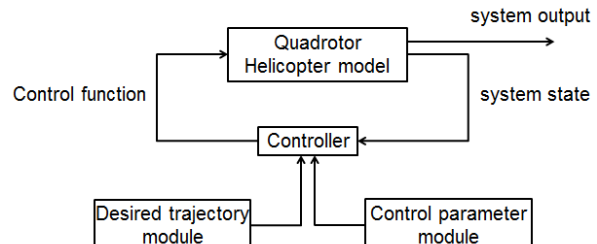


Figure 6. Schematic figure of simulation system module

The parameter of input for the system is $U = [U_1, U_2, U_3, U_4]^T$, which respectively are vertical tension, pitching tension, roll tension, and yaw pull force. System output is $Y = [Z, \phi, \theta, \psi]^T$, which are respectively z axis speed, pitch angle, roll angle, yaw angle. Some of the basic parameters for QballX4 quad-rotor UAV model simulation are shown in Table I.

The Matlab Control System Toolbox provides complete commands and algorithms for solving linear two-order optimal control problems. Normally, if the desired input signal is small, select the larger R matrix, which forces the input signal to be smaller. Otherwise, the objective function will increase and will not achieve the optimization requirements. Step signals are added to the control system, and then the parameters of the PID are adjusted. With repeatedly adjusting the PID parameter, we get the most desirable PID parameter. The parameters of the final selected Q, R, and scheduled P, I, and D for controllers of each parameter are shown in table II for the path tracking mission.

TABLE I. BASIC PARAMETERS OF THE QUAD-ROTOR UAV QBALL-X4

Parameter	value
K	120N
ω	15rad/sec
J_x	0.03kg.m ²
J_y	0.03kg.m ²
J_z	0.04kg.m ²
m	1.4Kg
K'	4N.m
L	0.2m
g	9.8N/kg

TABLE II. CONTROLLER SIMULATION PARAMETERS

parameter	X/Y	Z	Pitch/roll	Yaw
Q	$diag([5,2, 0, 0.1])$	$diag([1,0, 50])$	$diag([100,0,2, 2000,10])$	$diag([1, 0.1])$
R	50	500000	30000	1000
P	0.362	0.013	0.062	0.032
I	0.045	0.010	0.018	
D	0.382	0.009	0.013	0.015
Actuator	0.439		1.107	

For the fault tolerant hovering mission with only single GS-PID controller for the height parameter Z implemented, according to the percentage of failure rate injected into the actuator, the fault condition of the system is divided into following 4 sections: 0~5% total lift drop, 5~10% total lift drop, 10~15% total lift drop and 15~20% total lift drop. The corresponding gain is scheduled in each section, and gain scheduling table is shown in Table III.

TABLE III. GAIN SCHEDULING TABLE

Fault section	failure rate	K_p	K_d	K_i
1	0~5%	0.362	0.162	0.315
2	5~10%	0.380	0.168	0.335
3	10~15%	0.386	0.170	0.348
4	15~20%	0.410	0.172	0.355

IV. SIMULATION RESULTS

A. Fault Tolerant Control of GS-PID Controller

When the Quanser Qball-X4UAV is hovering stable and the actuator fault is injected, the simulation results of UAV altitude with single PID controller and with GS-PID controller were compared.

Fig. 7 shows the height change of the UAV when the 7% actuator fault is injected with PID controller. It could be seen that the height of the drop is about 15.1 cm. After the 4.9s, the UAV is restored to the balance position with PID controller.

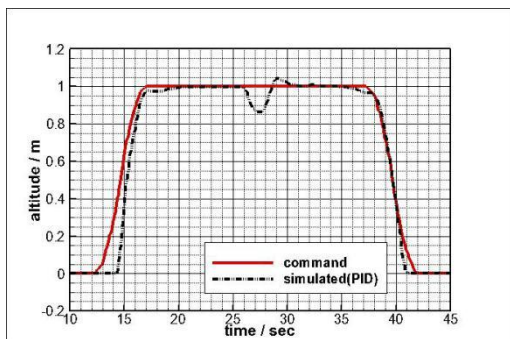


Figure 7. Height change for 7% actuator fault with single PID controller

Fig. 8 shows the height change of the UAV when the 7% actuator fault is injected with GS-PID controller. It could be seen that the height of the drop is about 7.2 cm. After the 3.1s, the UAV is restored to the balance position with GS-PID controller.

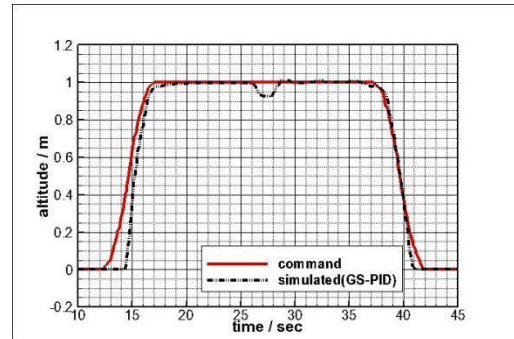


Figure 8. Height change for 6% actuator fault with single GS-PID controller

Fig. 9 shows the height change of the UAV when the 13% actuator fault is injected with single PID controller. It could be seen that single PID is unable to control the UAV to return to the equilibrium position. Because when the fault is injected, the aerodynamic force generated by the four propellers will be smaller than the gravity of the UAV, and the speed of the UAV will decrease quickly. The single PID output control is unstable, so aircraft begin oscillation. Certainly, the ability of UAV to restore steady state is related with the throttle limit of motors. The limited amplitude of the output of the PID controller and the low voltage of the battery will weaken the ability of the aircraft to recover the steady state.

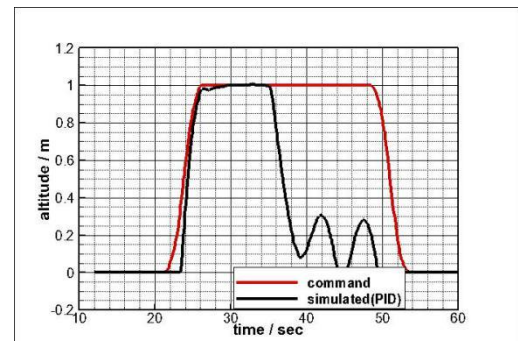


Figure 9. Height change for 13% actuator fault with single PID controller

Fig. 10 shows the height change of the UAV when the 13% actuator fault is injected with GS-PID controller. It could be seen that the height of the drop is about 13.1 cm. After the 7.2s, the UAV is restored to the balance position with GS-PID controller. Although there is a small overshoot, it makes the UAV's drop decrease and restore to the steady state. Therefore, compared with the single PID, the GS-PID can deal with the fault state better, and has better fault-tolerant control performance. The GS-PID control method reduces the time and the amplitude of the UAV to recover the steady state, and can handle the larger actuator faults.

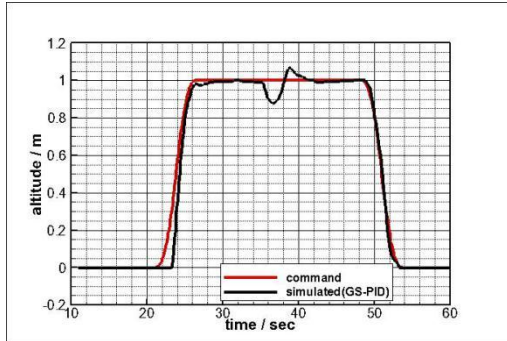


Figure 10. Height change for 13% actuator fault with single GS-PID controller

B. Trajectory Tracking Control with GS-PID controller

A trajectory tracking control is performed by the simulation system. Set the desired trajectory for the trajectory tracking control as,

$$\begin{aligned}x_d &= \sin t(1 - e^{-t^3}) \text{ (m)} \\y_d &= \sin t(1 - e^{-t^3}) \text{ (m)} \\z_d &= \sin t(1 - e^{-t^3}) \text{ (m)}\end{aligned}$$

and desired yaw angle trajectory is

$$\psi_d = 30 \sin t(1 - e^{-t^3}) \text{ (deg)}$$

The attenuation term is used to ensure that the derivative of the desired trajectory is zero at zero time. In a very short period of time, the expected output is attenuated:

$$x_d = \sin t \text{ (m)}, y_d = \cos t \text{ (m)}, z_d = 1 \text{ (m)}$$

$$\psi_d = 30 \sin t \text{ (deg)}$$

Take the controller parameters as:

$$\begin{aligned}A_1 = A_2 = A_3 = A_4 &= \text{diag}[2,2] \\A_5 = A_6 = A_7 = A_8 &= 2 \\A_9 &= \text{diag}[2,2,2,2]\end{aligned}$$

In figures 11, 12 and 13, curves x , y , and z represent position output curves under trajectory tracking control, x_d , y_d , z_d represent the corresponding desired trajectory, and θ_x , θ_y , θ_z showed the error curve. As can be seen from the figures, the final error of the position output tends to zero, that is to say, the controller ensures the stability of the position output and achieves trajectory tracking. The adjustment time is about 3 seconds.

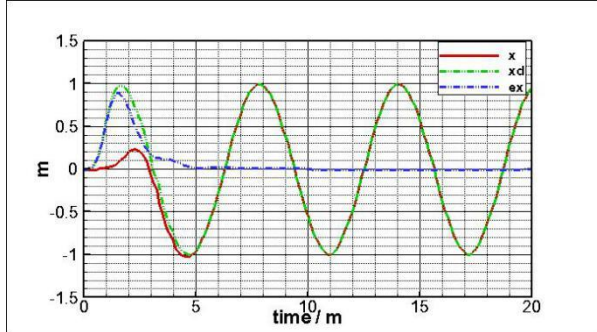


Figure 11. Position x under trajectory tracking, desired trajectory x_d and its error curve

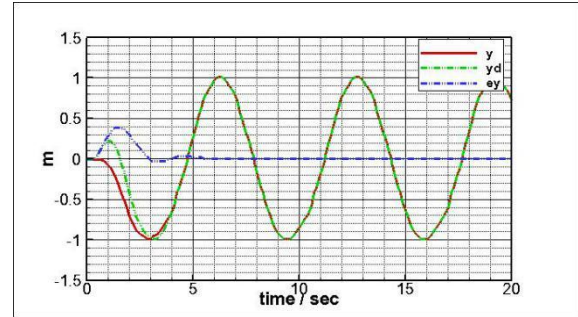


Figure 12. Position y under trajectory tracking, desired trajectory y_d and its error curve

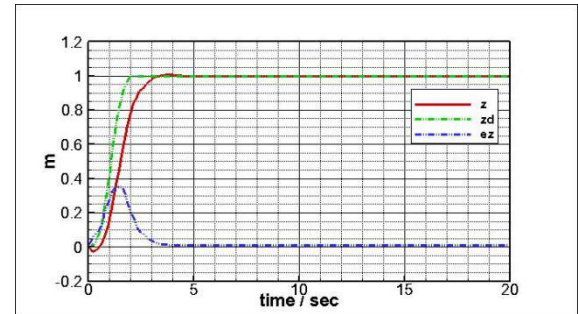


Figure 13. Position z under trajectory tracking, desired trajectory z_d and its error curve

Fig. 14 shows yaw trajectory, ψ_d is the desired trajectory yaw angle, e_ψ showed the corresponding error. It can be seen that after the system is stable, e_ψ is vibration up and down at 2 degrees that is to say the system tracking error is less than 6.7%. The trajectory tracking of yaw angle is achieved.

Figs. 15 and 16 show the output curve of the system roll angle ϕ and pitch angle θ . As you can see from the figures, the roll angle and pitch angle tend to be stable in 5 seconds and vibrate at a maximum of 5 degrees. The magnitude of this vibration is acceptable in practice.

The simulation results indicate that in the trajectory tracking control, the state of system x, y, z, ψ is to track the desired trajectory, while keep the attitude angle $\{\phi, \theta\}$ steady. The simulation results also indicated that the system control force for trajectory tracking is eventually stabilized at about 5 second, no more than 40 Newton within normal range, and the resultant composition forces is eventually stabilized near 19.6 newton, which is exactly the weight of the aircraft.

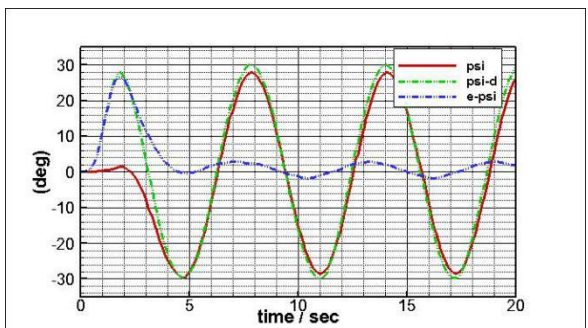


Figure 14. Yaw angle ψ under trajectory tracking, desired yaw angle ψ_d and its error curve

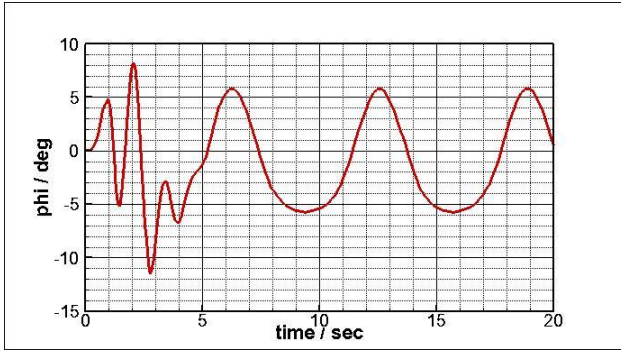


Figure 15. Curve of rolling angle ϕ under trajectory tracking

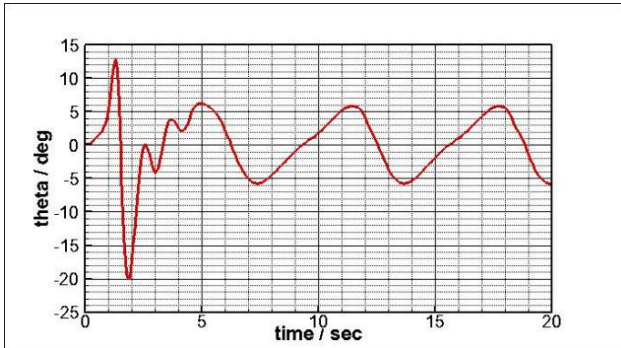


Figure 16. Curve of pitching angle θ under trajectory tracking

Figure 17 is a three dimensional trajectory map of a Quad-Rotor unmanned aerial vehicle (UAV) trajectory tracking. As can be seen from the figure, the aircraft starts at points $(0, 0, 0)$, then spirals up to the plane of $z=1$, and this plane travels along a circle of 1 meters in diameter. Therefore, the control design makes the Quad-Rotor UAV achieve the trajectory tracking effect.

In order to further illustrate the dynamics control of the Quad-rotor UAV with present GS-PID controller, the control force and the torque under trajectory tracking are all shown in the following figures.

Figs. 18, 19, 20 and 21 show the results of the system control force for trajectory tracking. It can be seen from figure 14, 15, 16 and 17 that, the control forces of the system, F_1, F_2, F_3, F_4 , eventually stabilized at about 5 second, no more than 40 Newton within normal range.

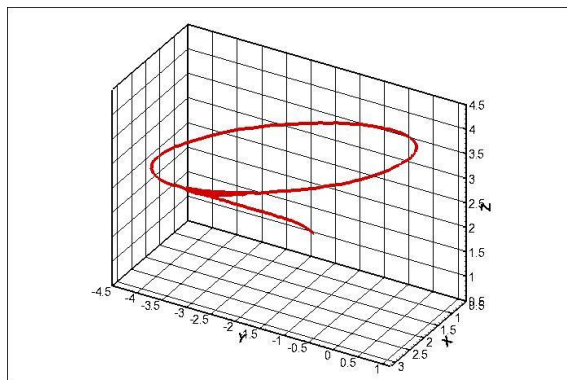


Figure 17. 3D rendering of trajectory tracking

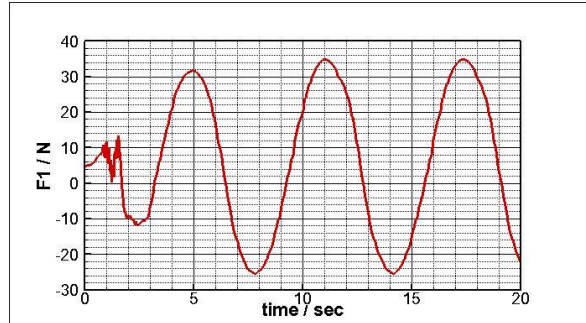


Figure 18. Trajectory tracking control force curve F_1

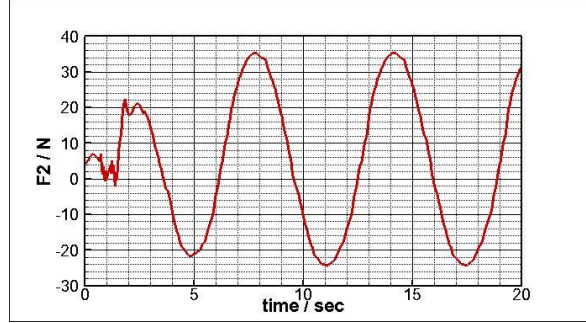


Figure 19. Trajectory tracking control force curve F_2

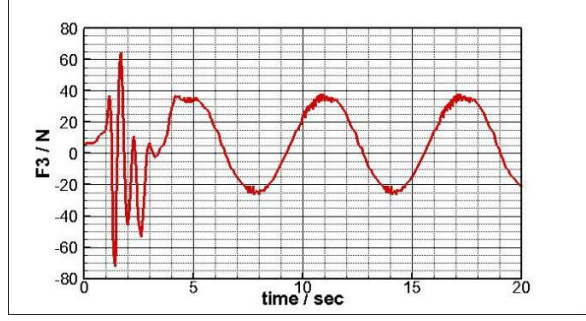


Figure 20. Trajectory tracking control force curve F_3

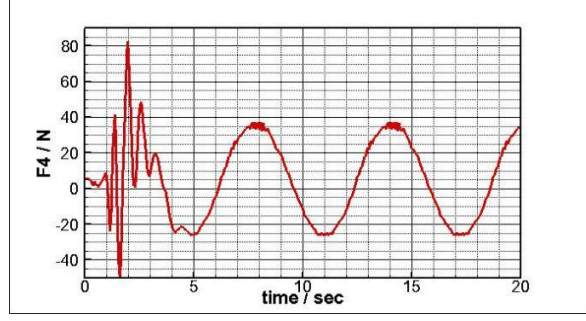


Figure 21. Trajectory tracking control force curve F_4

V. CONCLUSIONS AND FUTURE WORKS

A. Conclusions

In this paper, robust GS-PID control strategies were presented for the control of quad-rotor UAV in both missions. The proposed controller has been implemented in a nonlinear six-degree of freedom simulation model of a quad-rotor UAV.

Using the simulation, it is found that the GS-PID controller can achieve an excellent performance, and the model analysis, work point selection method and gain

scheduling PID controller design presented in this paper is effective for the fault-tolerant control and the path tracking of the quad-rotor UAV. The simulation results show that the PID control structure for the quad-rotor UAV could increase the performance of the quad-rotor UAV in tracking the desired trajectory and increases reliability of the UAV. Based on the proposed pre-tuned controller gain design, advantages (for example, robust properties, easy design and implementation) of GS-PID controller can be employed and the drawback of lack of tuning of PID controller gains is avoided.

B. Future Works

Future works concerning implementing GS-PID control to multiple missions on a quad-rotor UAV, and adopting Fault Tolerant Control process in a complete flight mission of the quad-rotor UAV will be taken place.

A potential application of the GS-PID controller is the controlling of the payload dropping and payload carrying of a quad-rotor UAV in flight. In order to obtain the best stability and performance of Qball-X4 under both payload carrying and payload dropping conditions, especially in payload dropping scenario, the switching action from one set of PID gains to another plays a vital role in performance of the helicopter at the moment of releasing the payload. In other words, if this transient (switching) time is held long (more than one second), it can cause the Qball-X4 to overshoot abruptly and even a crash. This payload dropping and payload carrying using a quad-rotor UAV based on GS-PID control algorithms will be presented in future paper.

ACKNOWLEDGMENT

The authors wish to thank all colleagues in the Diagnosis, Flight Control and Simulation Lab (DFCSL) and Networked Autonomous Vehicles Lab (NAVL) at Concordia University for providing support with experiment and computation.

REFERENCES

- [1] Y. M. Zhang, A. Chamseddine, C. A. Rabbath, B. W. Gordon, C.-Y. Su, S. Rakheja, C. Fulford, J. Apkarian and P. Gosselin, "Development of advanced FDD and FTC techniques with application to an unmanned quad-rotor helicopter testbed," *J. Franklin Inst.*, vol. 350, no. 9, pp. 2396-2422, Sep. 2013.
- [2] F. Lin, K. Z. Y. Ang, F. Wang, B. M. Chen, T. H. Lee, B. Yang, M. Dong, X. Dong, J. Cui, S. K. Phang, B. Wang, D. Luo, K. Peng, G. Cai, S. Zhao, M. Yin and K. Li, "Development of an unmanned coaxial rotocraft for the DARPA UAV Forge challenge," *Unmanned Syst.*, vol. 1, no. 2, pp. 211-245. Jan. 2013.
- [3] Soldiers Magazine, Quanser's Rapid Control prototyping (QuaRC), Available: <http://www.quanser.com/quarc> (Accessed on 3 November 2012).
- [4] P. Castillo, P. Garcia, R. Lozano, P. Albertos. Modelado y Estabilización de un Helicóptero con cuatro motores. Revista Iberoamericana de Automática e Informática Industrial RIAI, ISSN: 1697-7912 4, 41-57, July 2007.
- [5] G. V. Rao, M. G. Ortega, F. R. Rubio, "Robust Backstepping/Nonlinear H1 control for path tracking of a quad-rotor unmanned aerial vehicle," *Proceedings American Control Conference (Acc'08) Seattle*. Wa. USA, 2008.
- [6] K. Alexis, G. Nikolakopoulos and A. Tzes, "Model predictive control scheme for the autonomous flight of an unmanned quad-rotor industrial electronics (ISIE)," *2011 IEEE International Symposium on* 2243-2248, June 27-30, 2011
- [7] M. Chen, M. Huzmezan A Combined MBPC/2 DOF H Controller for a Quad Rotor UAV Proc. AIAA Guidance, Navigation, and Control Conference and Exhibit Texas, USA, August 11-14, 2003.
- [8] M. Chen, M. Huzmezan, "A simulation model and H_∞ loop shaping control of a quad rotor unmanned air vehicle," in *Proc. Iasted International Conference on Modelling, Simulation and Optimization - Mso 2003*, Banff, Canada, 320-325, July. DBLP, 2003
- [9] E. Altug, J. P. Ostrowski, R. Mahony, "Control of a Quad-rotor helicopter using visual feedback robotics and automation," in *Proc. ICRA '02. IEEE International Conference on 2002. Proceedings*, vol. 1 72 -77, May 2002
- [10] A. Wahyudie, T. B. Susilo and H. Noura, "Robust PID controller for quad-rotors," *J. Unmanned Syst. Technol.*, vol. 1, no. 1, pp. 14-19, Jan. 2013.
- [11] A. Bani Milhim, Y. Zhang, and C. A. Rabbath, "Gain scheduling based PID controller for fault tolerant control of a quad-rotor UAV, AIAA Infotech@Aerospace 2010," 20-22, Atlanta, Georgia, AIAA 2010-3530, April 2010.
- [12] I. Sadeghzadeh, M. Abdolhosseini, Y. Zhang, "Payload drop application using an unmanned quadrotor helicopter based on gain-scheduled PID and model predictive control," *Unmanned Systems*, vol. 2, no. 1, pp. 39-52, Jan. 2014.
- [13] W. J. Rugh, J. S. Shamma, "A survey of research on gain-scheduling," *Automatica* 36, pp. 1401-1425, 2000.
- [14] D. J. Leith and W. E. Leithead, "Survey of gain-scheduling analysis and design," *International Journal of Control*, vol. 73, no. 11, pp. 1001-1025, 2000
- [15] M. Mohammadi, A. M. Shahri, Z. Boroujeni, "Modeling and adaptive tracking control of a DOI 10.5013/ IJSSST .a.17.29.22," ISSN: 1473-804x online, 1473-8031 print.
- [16] "Quadrotor UAV," *International Journal of Intelligent Mechatronics and Robotics*, vol. 2, no. 4, pp. 58-81, October-December 2012.
- [17] X. Liang, G. D. Chen, J. H. Wang, Z. Y. Bi, P. Sun, "An adaptive control system for variable mass quad-rotor UAV involved in rescue missions," DOI 10.5013/ IJSSST .a.17.29.22, ISSN: 1473-804x online, 1473-8031 print.



Jing Qiao, a post-graduate student in the Department of Mechanical, Industrial and Aerospace Engineering of Concordia University, Montreal, Canada. Received Bachelor's degree from the Northwestern Polytechnical University, Xi'an, China in 2014, Majoring in automation.

Currently in the Master of Applied Science degree program in Concordia University. Research works focused on flight control techniques and unmanned systems control algorithms.



Zhixiang Liu, a post-doctoral research associate in the Department of Mechanical, Industrial and Aerospace Engineering of Concordia University, Montreal, Canada. Received PhD degree from Concordia University in 2012. Research works includes Guidance, navigation and control(GNC) of unmanned systems, fault detection, diagnosis and tolerant control of system failures.

Yomin Zhang, a full professor in the Department of Mechanical, Industrial and Aerospace Engineering of Concordia University, Montreal, Canada.